

Study on cavitation influence for pump head in an axial flow pump

K Hosono¹, Y Kajie¹, S Saito² and K Miyagawa²

¹ Graduate School, Department of Applied Mechanics, WASEDA University,
3-4-1 Okubo, Shinjuku-ku, Tokyo 168-8555, Japan

² Department of Applied Mechanics and Aerospace Engineering,
WASEDA University, 3-4-1 Okubo, Shinjuku-ku, Tokyo 168-8555, Japan

E-mail: hoppi-kazu@fuji.waseda.jp

Abstract. The size of axial flow pumps used in drainage pump stations has recently decreased, and their rotation speeds have increased, causing an increase in the risk of cavitation. Therefore, to provide highly reliable pumps, it is important to understand the internal flow of pumps under cavitating conditions. In this study, high-speed camera measurements and computational fluid dynamics analysis were performed to understand the cavitation performance of an axial flow pump. The mechanism that causes the head to change as a result of cavitation under low net positive suction head values is shown to be the balance between the increasing angular momentum and the loss indicated by the changing streamlines.

1. Introduction

Recently the size of axial flow pumps has decreased, and their rotation speeds have increased. This has caused an increase in the risk of cavitation, which causes performance degradation. Therefore, to provide highly reliable pumps, it is important to understand the internal flow under cavitating conditions.

Many studies have proposed methods of determining the internal flow of axial flow pumps under cavitating conditions. Using experimental measurements of an axial flow pump under cavitating conditions, Saito [1] showed that impeller outlet flow is affected by the occurrence of cavitation at the impeller. Goltz *et al* [2] examined the performance of an axial flow pump and showed a difference in cavitation due to the flow rate. Zheng *et al* [3] discussed the tip leakage flow of an axial flow pump based on their experiments and computational fluid dynamics (CFD) analysis and showed that the tip leakage vortex is influenced by the blade loading and operation conditions.

Thus, the influence of cavitation on pump performance has already been studied, meaning the internal flow in an axial flow pump has been measured. However, the mechanisms that cause the change in performance have not yet been clarified. Through the results of experiments and CFD analysis, this paper reveals the mechanisms that change the performance of an axial flow pump when cavitation occurs.

2. Experimental apparatus and computational fluid dynamics analysis

2.1. Experimental apparatus and procedures

Figure 1(a) shows the axial flow pump test apparatus in the closed-loop water tunnel. The diameter of the pipes at the test section is 145 mm, and that elsewhere is 155.4 mm. The test impeller is shown in figure 2. The number of impeller blades is 4, and the specific speed of this impeller at the best efficiency point is $N_s = 1400$ [m, m³/min, rpm]. The diameter of the impeller is 144.4 mm, and the clearance between the impeller tip and the casing is 0.3 mm. The casing of the test section, which is shown in



figure 1(b), is made of acrylic glass, allowing the internal flow and cavitation to be visualized. The net positive suction head (NPSH) can be changed by the vacuum pump connected to the upstream tank for cavitation tests.

The flow rate is changed by the valve at the discharge side of the pump and the flow rate is measured by a magnetic flowmeter. The head is calculated from the differences in the static and dynamic pressures caused by changing the cross sectional area. Moreover, the shaft power is computed by a torque meter at the impeller shaft. The internal flow and cavitation are imaged by a high-speed digital video camera. The frame rate of this camera is set to 1000 fps.

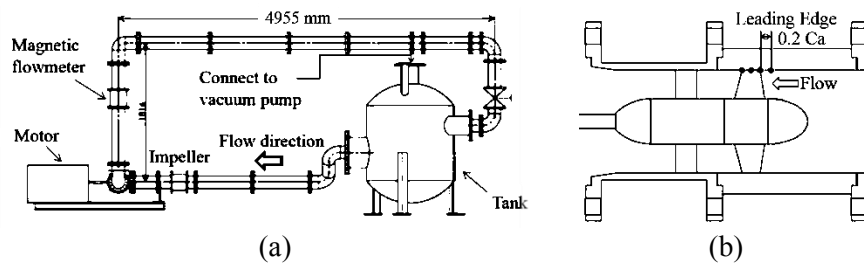


Figure 1. Axial flow pump test apparatus. (a) Overview of apparatus, (b) test section of axial flow pump.

Figure 2. Test impeller.

2.2. Pump performance and cavitation characteristics

Figure 3(a) shows the efficiency, the head coefficient Ψ , and the shaft power coefficient ν with respect to the nondimensionalized flow rate Q/Q_d at the design point; these graphs represent the performance curves of the axial flow pump. There is a monotonic decrease in the head coefficient from the shut point to $Q/Q_d = 0.7$, followed by an increase in the range $Q/Q_d = 0.7-0.85$ as a positive-slope characteristic. Figure 3(b) shows cavitation characteristics of the head coefficient Ψ with respect to NPSH. At the design point flow rate, the head coefficient achieves a maximum value at nearly NPSH = 2.2 m. Conversely, there are no peaks for flow rates less than the design point flow rate.

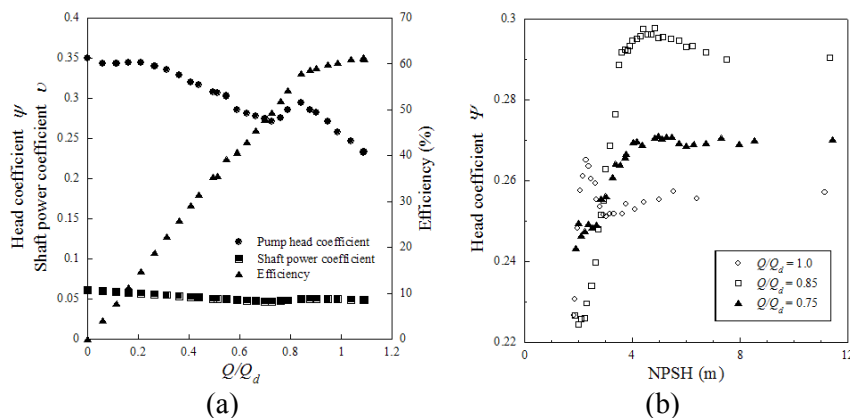


Figure 3. (a) Experimentally obtained performance curves and (b) cavitation characteristics of the axial flow pump.

2.3. Computational fluid dynamics analysis and procedures

In this study, the commercial CFD code ANSYS CFX 14.5 is used. The computational grid consists of approximately 4.2 million hexa-elements and 4.3 million nodes. There are 20 layers in the tip clearance. In this CFD analysis, the standard k- ϵ model is used as the turbulence model, and the simplified Rayleigh-Plesset based model in ANSYS CFX is used as the cavitation model. The boundary conditions of constant total pressure and constant mass flow rate are set at the inlet and outlet, respectively.

3. Result and discussion

3.1. Comparison of computational fluid dynamics analysis and experimental results

Figure 4 shows the cavitation characteristics of the axial flow pump obtained experimentally and by CFD analysis at the design point. The CFD analysis and experiments are in good agreement and both have a maximum head coefficient point at NPSH = 2.2 m. Therefore, the internal flow under cavitating conditions can be simulated by CFD analysis with high accuracy.

The photographs on the left of figure 5 show the cavitation at the design point for NPSH values of 6.3 m and 4.2 m. Vortex cavitation occurs at NPSH = 6.3 m, and both vortex and sheet-type cavitation occur at NPSH = 4.2 m. The images on the right in figure 5 show the visualization of the cavitation area (void fraction = 0.1) obtained by CFD analysis. In the case of NPSH = 4.2 m, the sheet-type cavitation can be simulated, but the vortex cavitation cannot.

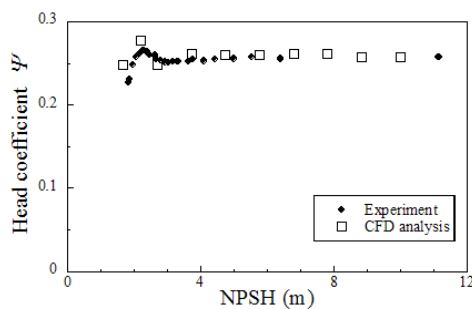


Figure 4. Cavitation characteristics obtained experimentally and by CFD analysis at the design point.

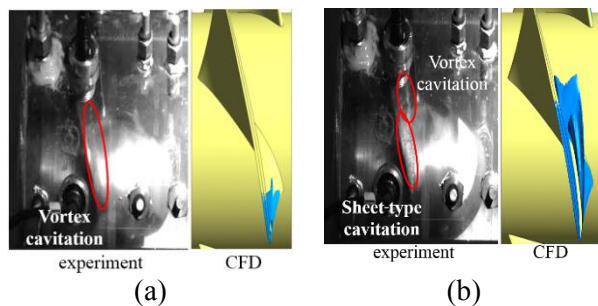


Figure 5. Visualization of cavitation at the design point for NPSH = (a) 6.3 m (b) 4.2 m.

3.2. Head coefficient changing under low net positive suction head

Figure 6 shows the distributions of the pressure coefficient and the angular momentum from the front to the back of the impeller obtained by CFD analysis at the design point. In the pressure coefficient distribution, it is linked to the head coefficient changing. However, the angular momentum increases with decreasing NPSH, especially in the shroud. Under these conditions, the angular momentum is highest at NPSH = 1.8 m, but the pressure coefficient is highest at NPSH = 2.2 m.

The impeller blade loading distribution from leading edge (L.E.) to trailing edge (T.E.) at the hub and the shroud are shown in figure 7. At the hub, CFD analysis shows that the blade loading is largest at NPSH = 1.8 m. By contrast, the blade loading values at NPSH = 1.8 m and 2.2 m in the shroud are almost equal. In spite of this, the head coefficient is highest at NPSH = 2.2 m. This demonstrates that changes in the head coefficient do not correspond to changes in the impeller blade loading distribution.

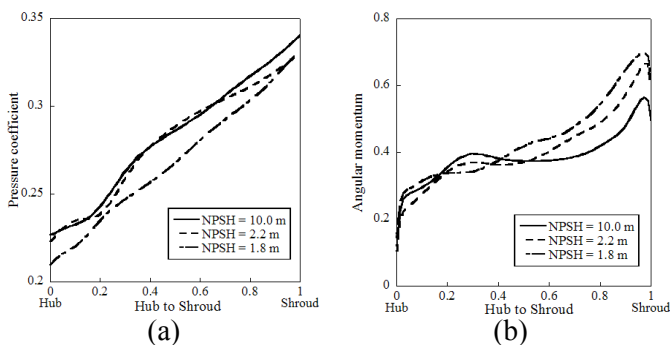


Figure 6. Distributions of (a) the pressure coefficient and (b) the angular momentum at the design point.

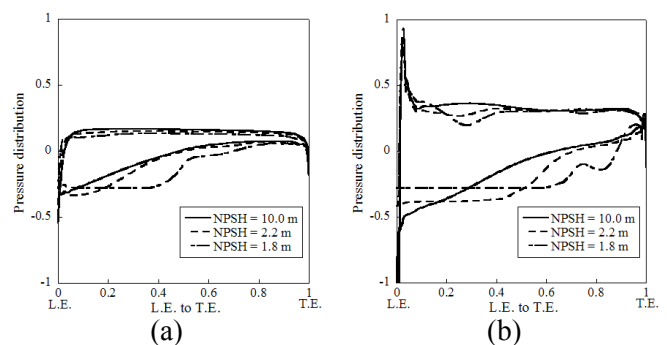


Figure 7. Impeller blade loading at (a) the hub and (b) the shroud at the design point.

3.3. Mechanisms of head coefficient changing under low net positive suction head

Figure 8 shows the average loss coefficient at the pump meridional plane obtained by CFD analysis at the design point. The loss coefficient (L.C.) is defined as the nondimensionalized relative total pressure decrease from the inlet value. The high loss coefficient area increases as the NPSH becomes smaller. The loss caused by the tip leakage flow is high near the shroud area. Moreover, near the hub area, the loss caused by the cross sectional flow due to cavitation is higher at low NPSH values.

Figure 9 shows the streamlines obtained by CFD analysis on the suction side of the blade. Comparing the streamlines for NPSH = 2.2 and 1.8 m indicates that the position of the cross sectional flow moves downstream with decreasing NPSH. The pump head changing due to cavitation is the result of the balance between the increasing angular momentum and the loss indicated by the streamlines changing.

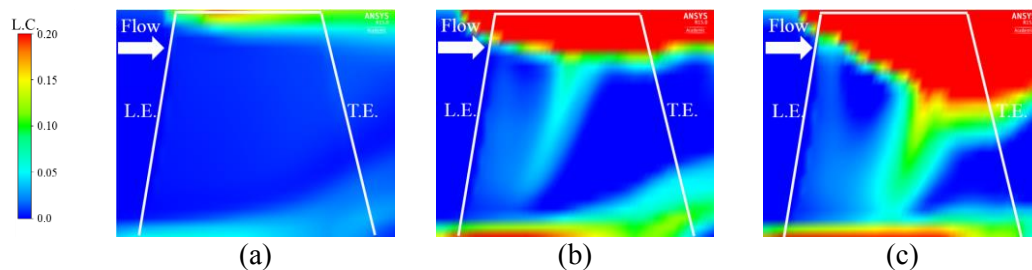


Figure 8. Loss coefficient contour at the meridional plane at the design point for NPSH = (a) 10 m, (b) 2.2 m, (c) 1.8 m.

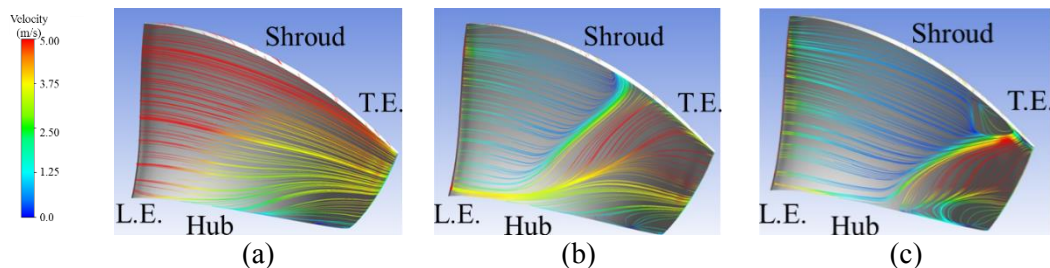


Figure 9. Streamlines at the blade surface suction side at the design point for NPSH = (a) 10 m, (b) 2.2 m, (c) 1.8 m.

4. Conclusion

The results obtained from this study are as follows.

- (1) The angular momentum increases with decreasing NPSH under cavitating conditions. However, changes in the pressure and head coefficients do not correspond to increasing angular momentum.
- (2) With decreasing NPSH, the high loss coefficient area caused by the tip leakage and cross sectional flows due to cavitation increases.
- (3) The changes in the pump head due to cavitation are the result of the balance between the increasing angular momentum and the loss indicated by the changing streamlines.

References

- [1] Saito S 1987 Cavitation Aspect and Flow Pattern in an Axial-Flow Impeller *T. JSME B* **53-492** pp 3682-90
- [2] Gortz I, Kosyna G, Stark U, Saathoff H and Bross S 2003 Stall inception phenomena in a single-stage axial-flow pump *Proc. IMechE* (Braunschweig, Germany) pp 471-79
- [3] Zhang D, Shi W, Esch B, Shi L and Dubuisson M 2015 Numerical and experimental investigation of tip leakage vortex trajectory and dynamics in an axial flow pump *Computers & Fluids* **112** pp 61-71